

Molecular pendular states in intense laser fields

G. Ravindra Kumar, P. Gross, C. P. Safvan, F. A. Rajgara, and D. Mathur
Tata Institute of Fundamental Research, Homi Bhabha Road, Bombay 400 005, India

(Received 22 June 1995; revised manuscript received 27 December 1995)

Direct experimental evidence is presented for the formation of aligned states of the linear triatomic molecules CO_2 and CS_2 ; manifestation of pendular motion is obtained in high-resolution measurements of the angular distributions of fragments produced by an intense laser-field–molecule interaction. Classical calculations of the dissociation dynamics on an excited-state potential-energy surface yield results that qualitatively reproduce our experimental observations.

PACS number(s): 33.20.–t, 33.15.–e, 33.55.–b, 33.80.–b

I. INTRODUCTION

The interaction of a molecule with the electric-field vector of intense, polarized, laser radiation can induce a dipole moment that is sufficient to result in the creation of aligned, inertially trapped molecules. Picosecond and subpicosecond laser pulses producing field strengths of the order of 10^{14} W cm^{-2} have been utilized to study dissociative multiple ionization of diatomic molecules aligned in such manner [1,2]. Recent calculations [3] have indicated that aligned pendular states that arise out of laser-field-induced dipole moments are directional superpositions of field-free molecular states, corresponding to oblate spheroidal wave functions, whose eigenenergies are inversely proportional to field strength. The prospect of trapping molecules [3,4], aligning them, and subjecting them to inertial confinement [1,3,5] by means of a polarization interaction with an intense laser beam opens horizons for a class of ultrahigh-resolution and high-precision spectrometric and collisional experiments of the type hitherto applicable only to *charged* atoms and molecules in electromagnetic traps.

We report here the results of high-resolution measurements of the angular distributions of singly charged fragments arising from the interaction of linear triatomic molecules CO_2 and CS_2 with 30-ps pulses of 532-nm radiation at intensities of 10^{13} – 10^{14} W cm^{-2} ; a considerable enhancement of angular resolution accompanied by measurement of the pristine angular distributions has facilitated the direct observation of intense-field-induced aligned states of *thermal-energy* molecules. These states exhibit pendular motion that manifests itself as *structure* in the strongly anisotropic angular distributions of dissociation products; such distributions are qualitatively reproduced in a classical model of the dissociation dynamics on an excited molecular potential-energy surface.

The alignment of CO_2 and CS_2 molecules has been studied by measuring the angular distributions of fragment ions that arise out of the interaction of these linear triatomic molecules with an intense laser field. Our recent studies [6] have shown that the fragmentation dynamics of these molecules, at 532 nm and at the intensity levels used in the present experiment, is marked by a preference for dissociation of the neutral parent molecule followed by ionization of fragments. The ion kinetic energies expected here are much lower than

those in “Coulomb explosion” studies of multiply charged molecules.

II. EXPERIMENTAL METHOD

The angular distributions were measured using a crossed-beam apparatus that has been described in recent reports on the competition between field-induced molecular dissociation and ionization [6] and only the salient features are described here. Focused, linearly polarized, 35-ps, 532-nm pulses (10-Hz repetition rate) from an Nd:YAG laser (where Nd:YAG denotes neodymium-doped yttrium aluminium garnet) interact with an effusive molecular beam in a field-free region and the resulting ions are mass analyzed by a quadrupole filter.

Ion angular distributions were measured by rotating the laser polarization vector with respect to the quadrupole filter’s axis; the final polarization state was selected using a linear polarizer, which was rotated in steps of 2° – 4° . The linearly polarized laser radiation was passed through a half-wave plate to rotate the polarization vector and to ensure that the final energy of the laser pulse was kept constant. The shot-to-shot reproducibility of the laser was $\pm 5\%$.

The unique feature of the present experiment is the *complete absence* of an electrostatic field to extract the ions into the mass filter; almost all earlier measurements have all utilized time-of-flight ion analysis techniques in which large extraction fields (of the order of 600 V cm^{-1}) are mandatory. Such fields result in distortions of the measured angular distribution functions, particularly those pertaining to multiply charged ions [5]. In our case, only those singly charged ions whose initial velocity vector lies within the acceptance angle set by the entrance aperture of the mass filter are detected; the best angular resolution achieved was $\pm 1.8^\circ$. Adequate precautions are taken to avoid saturation effects by keeping molecular beam densities low and restricting laser beam energies to values that avoid saturation of the detector.

III. RESULTS AND DISCUSSION

Our experimental results are shown in Figs. 1 and 2 as polar plots depicting the number of peripheral fragment ions as a function of the angle between mass filter’s axis and the light polarization vector. The angular distributions are markedly anisotropic, with the minimum ion intensity obtained

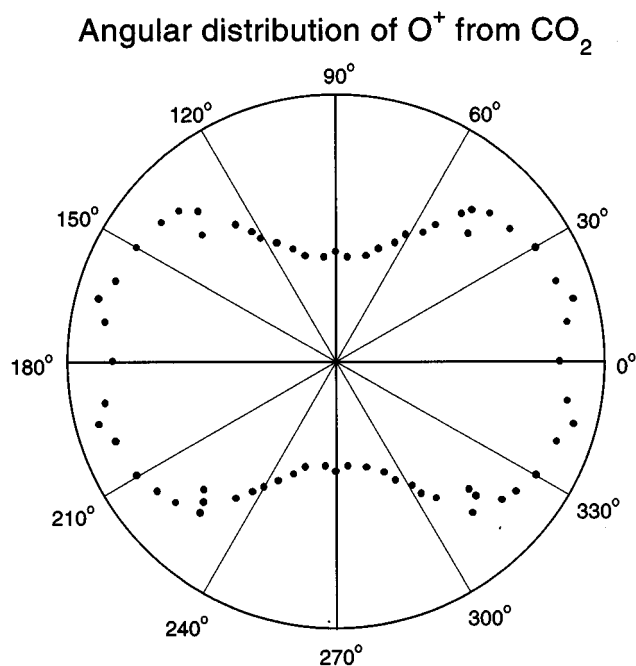


FIG. 1. Angular distribution of O^+ fragment ions arising from dissociation of CO_2 by a laser field at 532 nm, $10^{13} \text{ W cm}^{-2}$. The polarization axis of the incident radiation is horizontal (0°). The spot sizes are a measure of the radial uncertainty. The radial extent is from 0 to 300.

when the light polarization vector is orthogonal to the observation direction. The dynamic range of the signal in these experiments usually covered two orders of magnitude. For instance, typical counts for S^+ ions from CS_2 were of the order of 1000 at 0° and of the order of 30 at 90° , for counting times of 100 s (1000 laser shots). Although the count rate at 90° was small, typical signal-to-noise ratios were always in excess of 20.

For both fragment ions, there are indications of lobelike structure in the region of 10° – 15° . We have also carried out angular distribution measurements using different values of extraction field; it is found that even the smallest such field ($\leq 10 \text{ V cm}^{-1}$) results in serious distortions of the angular distributions, smearing any structural information. Figure 3 shows a typical angular distribution for S^+ ions from CS_2 measured with an extraction field of 8 V cm^{-1} : the marked anisotropy observed in the field-free case is almost totally destroyed.

Before considering these results in the light of model calculations that we have carried out, a qualitative overview of the dynamics of the molecule–intense-field interaction may be summarized as follows. In the course of the laser-molecule interaction, CO_2 and CS_2 , both of which are easily polarizable molecules, experience a significant torque even in the low-intensity, rising edge of the laser pulse. No matter what the initial orientation of the molecule, the induced dipole moment tends to rotate the molecular axis towards the polarization axis of the laser beam, and as the input field continues to increase, the C-X ($X=O,S$) bond lengths increase until an instant is reached at which dissociation takes place. The most significant implication of the field-induced dipole moment is that the molecules are

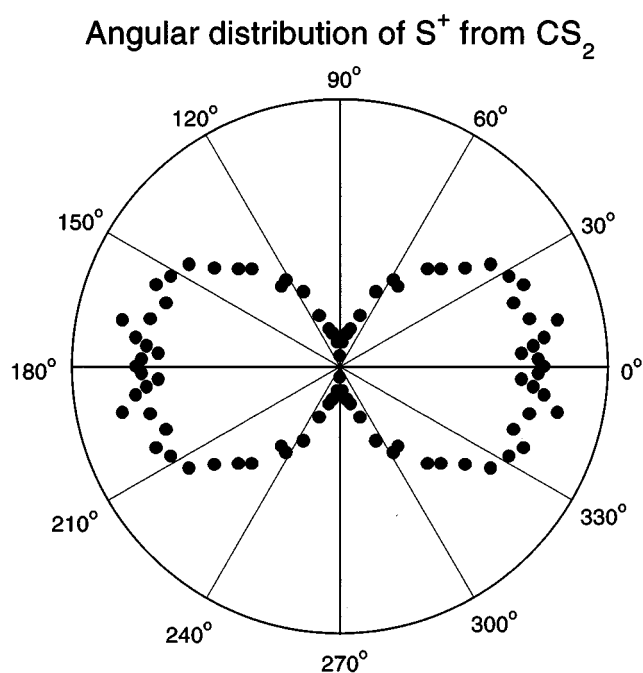


FIG. 2. Angular distribution of S^+ fragment ions arising from dissociation of CS_2 by a laser field at 532 nm, $10^{13} \text{ W cm}^{-2}$. The polarization axis of the incident radiation is horizontal (0°). The spot sizes are a measure of the radial uncertainty. The radial extent is from 0 to 200.

“trapped” in pendular states aligned about the field polarization axis, resulting in the anisotropic angular distribution.

Consider the dynamics under two extreme cases depicted schematically in Fig. 4: the molecule disintegrates when perfectly aligned with the polarization axis (minimum torque, maximum angular momentum) and when at the extreme of its pendular oscillations (maximum torque, zero angular momentum). In the former case the dissociation products will have a large component of velocity perpendicular to the molecular axis and hence there will be no fragments along the direction of the polarization axis. In the latter case, the molecule, having come to the extreme of its pendular motion, will have no velocity component perpendicular to the molecular axis and any fragments formed at this stage will be observed at the angle θ_{\max} . Taken in conjunction with the fact that the molecule spends more time around $\theta = \theta_{\max}$ than around $\theta=0$, we expect the fragment angular distribution to be strongly anisotropic, with a tendency to peak at θ_{\max} . The sharpness of the distribution is an indication not only of the polarizability of the molecule, its mass, and the strength of the light field, but also of the initial kinetic energy of the fragments. In this context it is of interest to note the significant differences between the CO_2 data and the angular distributions from the more polarizable CS_2 molecule (Figs. 1 and 2).

Our calculations assume a Franck-Condon transition between the molecular ground state and an excited (dissociative) potential-energy surface (PES) and model the subsequent dynamics classically. We also utilize the results of our earlier experiments, which indicate that at 532 nm, for both CO_2 and CS_2 , dissociation precedes ionization [6]. The oscillations of our laser field are neglected since the inverse of

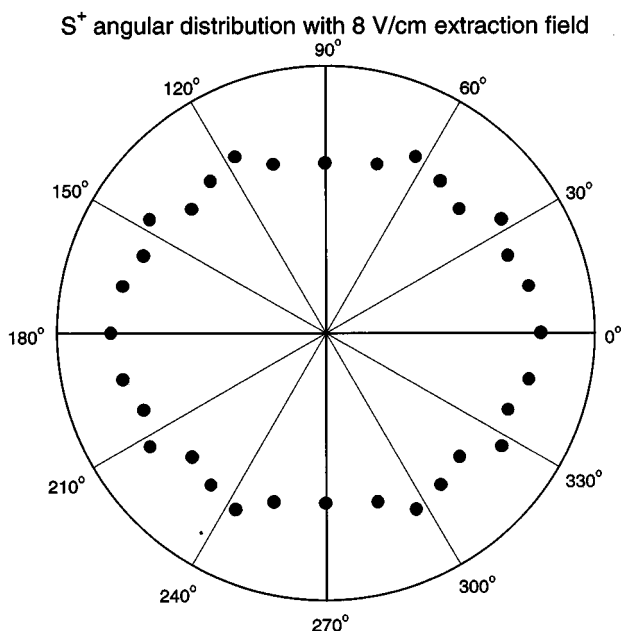


FIG. 3. Angular distribution of S^+ fragment ions arising from dissociation of CS_2 by a laser field at 532 nm, $10^{13} \text{ W cm}^{-2}$. An extraction field of 8 V cm^{-1} was applied in the course of these measurements. The polarization axis of the incident radiation is horizontal (0°).

the field frequency is much greater than length of the pulse [3] and “time-averaged” polarizabilities are assumed, which give rise to angular distributions that mimic the experimental data. The term “time-averaged” is used here because the polarizability changes with molecular bond length. However, since the functional dependence of the polarizability on bond length remains unknown, we take a time-averaged value that is adjusted to mimic experimental data.

The Hamiltonian for the system is written as

$$H = \frac{1}{2\mu} [p_1^2 + p_2^2] - \frac{p_1 p_2}{m_c} + V(r_1, r_2, \gamma_{\text{eq}}) + \frac{p_\theta^2}{2I} + V_\theta(\theta), \quad (1)$$

where r_1 and r_2 are the two C-X bond lengths (for convenience, we will hereafter refer only to the case of CO_2), θ is the angle between the molecular axis and that of the linearly polarized laser field, m_c is the carbon atom mass, μ is the reduced mass between the carbon and oxygen atoms, I is the moment of inertia of linear CO_2 , and γ_{eq} is the (fixed) equilibrium bond angle in CO_2 (180°). $V(r_1, r_2, \gamma_{\text{eq}})$, the excited-state PES that governs the dynamics, is a London-Eyring-Polyani-Sato (LEPS) surface (see Ref. [7] for the functional form) for which the parameters pertaining to CO_2 are provided in Ref. [8].

Photodissociation of CO_2 has been simulated quantum mechanically in both the time-dependent [9] and the time-independent [8] frames using these LEPS parameters. Asymptotically, in the limit of infinite separation (large r_1 or r_2), the LEPS surface corresponds energetically to $CO+O$ fragments. The total angular momentum of the molecules is

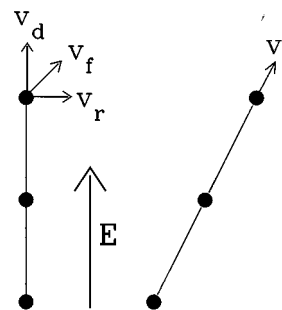


FIG. 4. Schematic representation of the dissociation dynamics of pendular states. Two cases are depicted: a molecule perfectly aligned with the laser polarization vector \vec{E} (left) and at the extreme (θ_{max}) of its pendular motion (right). v_d is the velocity component arising from the kinetic energy released upon dissociation, v_r is the rotational velocity of pendular motion, and v_f is the resultant. v_r has a maximum value when the molecular axis is parallel to \vec{E} and is zero at the extreme position.

coupled to the field through the molecular polarizability. For this the field-molecule interaction potential $V_\theta(\theta)$ is given by

$$V_\theta(\theta) = -\frac{1}{2} \epsilon^2 (\alpha_{\parallel} \cos^2 \theta + \alpha_{\perp} \sin^2 \theta), \quad (2)$$

where α_{\parallel} and α_{\perp} are the parallel the polarizability components parallel to and perpendicular to the molecular axis and ϵ is the average field strength. For linear triatomics such as CO_2 , $\alpha_{\parallel} > \alpha_{\perp}$. Here the average field strength (assuming a peak field intensity of $10^{13} \text{ W cm}^{-2}$) is taken as $8.7 \times 10^7 \text{ V cm}^{-1}$.

We integrate Hamilton’s equations for the three coordinates and their conjugate momenta, requiring initial conditions of $r_1, r_2, \theta, p_1, p_2, p_\theta$. For r_1 and r_2 we take a distribution of bond lengths for the initial conditions at time $t=0$, $r_1(0)$ and $r_2(0)$ [10]. To find these, our classical treatment demands that a radiative transition takes place only when there is an exact resonance between the ground and excited surfaces, i.e.,

$$V_e(r_1, r_2, \gamma_{\text{eq}}) - V_g(r_1, r_2, \gamma_{\text{eq}}) = n\hbar\omega, \quad (3)$$

where ω is the laser frequency and n is the photon number. Thus we determine the positions r_1 and r_2 for which Eq. (3) is satisfied and use these as our initial conditions. The photon number n in Eq. (3) here is 3 for a 532-nm wavelength. Indeed, strong absorption at this excitation energy has been experimentally observed in photodissociation spectra [11]. At some bond lengths four-photon transitions are also possible, but the bond lengths at these resonances are quite far from the ground-state potential equilibrium and therefore ignored since the wave-function amplitude far from the potential minimum is very small.

Ideally, each initial position should be weighted by the Wigner distribution corresponding to the ground-state vibrational wave-function. The initial momenta for the three coordinates must also be specified to integrate Hamilton’s equations. Since the Wigner distribution is strongly peaked

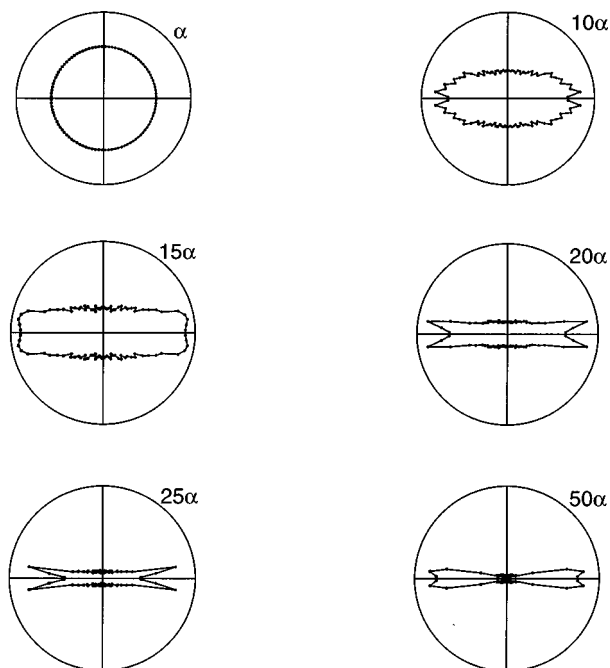


FIG. 5. Calculated angular distributions of O^+ from CO_2 with increasing time-averaged polarizabilities [10, 15, 20, 25, and 50 times the ground-state (zero-field) polarizability for CO_2 , $\alpha = 2.911 \times 10^{-24} \text{ cm}^3$]. Note the increasing alignment about the laser polarization axis (horizontal) with increasing polarizability, i.e., increasing field-molecule interaction. Also note the appearance of the heart-shaped peak at higher multiples of α .

at $p=0$, $p_1(0)=p_2(0)=0$. As for the initial total angular momentum, $p_\theta(0)$, we assumed that the molecules rotate with a single angular momentum $p_\theta(0) = \hbar \sqrt{J_{\max}(J_{\max} + 1)}$, where J_{\max} (≈ 16) is the most probable angular-momentum quantum number for CO_2 at 298 K.

With the above initial conditions specified at time $t=0$, Hamilton's equations were integrated for 600 different initial angles between the molecular and laser polarization axes [$\theta(0)$] and six initial vibrational bond lengths for each initial angle. These equations were integrated until a separation of $\sim 10 \text{ \AA}$ occurred between the CO and O fragments. For each trajectory, the final θ was recorded. After all trajectories, polar plots were created to show the angular distribution of products for various time-averaged polarizabilities of the excited-state surface (Fig. 5). These plots assume an angular

resolution of $\pm 1.8^\circ$.

Note that, with increasing polarizability, there is increasing alignment of fragment ions about the laser polarization axis, as expected. Also, the appearance of the "heart-shaped" distribution about the polarization axis, especially at higher values of polarizability (that is, higher field-molecule interaction energy). It is worth emphasizing that this is the first time, to our knowledge, that indications of such structure have been obtained in the fragment ion angular distribution in both the experimental results and the simulations.

Running the simulations at various polarizabilities is justified because the polarizability involved in this interaction is of a dynamic nature and can be substantially larger than its zero-field value (α). Molecules such as CS_2 display large nonlinearities, even at laser intensities as low as 10^7 – 10^8 W cm^{-2} [12], intensities attained in the rising edge of our laser pulse. In an intense-field situation, the polarizability will, in principle, have many nonlinear terms, each of which can be enhanced by resonances accessed. The sum total of all such terms can be orders of magnitude larger than α . Consequently, we anticipate large values of induced dipole moment in these interactions.

It is instructive to compare the (field-free) rotational energy (0.013 eV) of the linear CO_2 molecule at 298 K ($J=J_{\max} \approx 16$) with the field-molecule interaction energy [assuming $\theta=0$ in Eq. (2)], which is 0.193, 0.290, 0.386, 0.483, and 0.966 eV for the five polarizabilities assumed in Fig. 5. We note that the field-molecule interaction energy overwhelms the field-free rotational energy and thus can induce alignment.

IV. CONCLUSION

In summary, we have demonstrated the formation of aligned states of thermal-energy triatomic molecules in intense laser fields. Pendular motion manifests itself in the measured shapes of the angular distributions of dissociation products formed as a result of molecule-field interactions. The results of our dissociation dynamics model, using a LEPS potential energy surface, qualitatively reproduce the features of our data; the measured heart-shaped angular distributions are reproduced. The alignment that is measured fits in with the theory of Friedrich and Herschbach [3] and their interpretation of such alignment due to pendular states. We believe our measurements to be the most direct evidence for pendular motion of molecules in intense laser fields.

- [1] D. Normand, L.A. Lompré, and C. Cornaggia, *J. Phys. B* **25**, L497 (1992).
 [2] A. Zavriyev, P.H. Bucksbaum, H.G. Müller, and D.W. Schumacher, *Phys. Rev. A* **42**, 5500 (1990); D.T. Strickland, Y. Beaudoin, P. Dietrich, and P.B. Corkum, *Phys. Rev. Lett.* **68**, 2755 (1992); L.J. Frasinski, P.A. Hatherly, K. Codling, M. Larsson, A. Persson, and C.-G. Wahlström, *J. Phys. B* **27**, L109 (1994).

- [3] B. Friedrich and D. R. Herschbach, *Phys. Rev. Lett.* **74**, 4623 (1995).
 [4] G.R. Kumar, P. Gross, C.P. Safvan, F.A. Rajgara, and D. Mathur, *J. Phys. B* **29**, L95 (1996).
 [5] P. Dietrich, P.B. Corkum, D.T. Strickland, and M. Laberge, in *Molecules in Laser Fields*, edited by A.D. Bandrauk (Dekker, New York, 1994), p. 181. P. Dietrich, D.T. Strickland, M. Laberge, and P.B. Corkum, *Phys. Rev. A* **47**, 2305 (1993).

- [6] G.R. Kumar, C.P. Safvan, F.A. Rajgara, and D. Mathur, J. Phys. B **27**, 2981 (1994), Chem. Phys. Lett. **217**, 626 (1994).
- [7] J.T. Muckerman, J. Chem. Phys. **54**, 1155 (1971).
- [8] K.C. Kulander and J.C. Light, J. Chem. Phys. **73**, 4337 (1980).
- [9] R. Schinke and V. Engel, J. Chem. Phys. **93**, 3252 (1990).
- [10] R. Schinke, *Photodissociation Dynamics: Spectroscopy and Fragmentation of Small Polyatomic Molecules* (Cambridge University Press, Cambridge, 1993).
- [11] H. Okabe, *Photochemistry of Small Molecules* (Wiley, New York, 1978).
- [12] R.W. Boyd, *Nonlinear Optics* (Academic, Boston, 1992), Chap. 4.